JOURNAL OF SPACECRAFT AND ROCKETS
Vol. 48, No. 4, July–August 2011

Engineering Notes

Force Measurements in Hypervelocity Flows with an Acceleration Compensated Piezoelectric Balance

Eric C. Marineau*
CUBRC, Buffalo, New York, 14225

DOI: 10.2514/1.A32047

$\mathbf{C_A}$	=	acceleration weighting matrix
C_A	=	axial force coefficient
$\mathbf{C_F}$	=	force balance coefficient matrix
C_M	=	pitching moment coefficient about nose
C_N	=	normal force coefficient
$\mathbf{F(t)}$	=	force-and-moment vector
L/D	=	lift-to-drag ratio
N_A	=	number of accelerometer outputs
N_C	=	number of balance components
N_L	=	number of static load points
N_S	=	number of force sensors
$\mathbf{S_A(t)}$	=	accelerometer output vector
$\mathbf{S_F(t)}$	=	strain gage output vector

I. Introduction

THE effect of hypersonic gas chemistry modeling on the prediction of the pitching moment has recently been identified as a challenge for the Mars Science Laboratory entry descent and landing [1]. Expansion and reflected shock tunnels such as the LENS-XX and LENS-I facilities are the only type of facilities able to generate high enthalpy and Reynolds number flows required to study the effect hypersonic gas chemistry on vehicle forces and moments. In such tunnels, the short test time typically between 0.3 and 100 ms, offers no opportunity to completely damp the oscillations of the aerodynamic model and force measurement system. This makes direct force measurements challenging as the inertial forces resulting from the model and balance accelerations add to the aerodynamic forces. Force measurements data on reentry capsules at high enthalpy are very sparse [2,3] and display large uncertainties especially on the pitching moment. Recent measurements by Marineau et al. [4] have shown that it is possible to make accurate force measurements in shock tunnels with an acceleration compensated strain gage force balance. However, a new balance design is required to make accurate force measurements in the LENS-XX expansion tunnel due to the shorter test time (as low as 0.3 ms) and increased loads (up to 100 times). To address such challenges, a six-component acceleration compensated piezoelectric balance was designed, fabricated, calibrated, and tested in the 48 in. tunnel. Triaxial piezoelectric load cells are used in the new design due to their increased stiffness and load capacity compared with traditional flexures. Such piezoelectric transducers have been used successfully by Schewe and Steinhoff [5] for measurements of unsteady forces from vortex shedding behind a cylinder at very high Reynolds numbers (10E7) and by Norman [6] for unsteady forces on a sphere in the presence of a morphing surface. However, no use of triaxial piezoelectric load cells in short duration hypersonic tunnels has been reported in the literature. The primary objective of this paper is therefore to demonstrate the validity of this methodology in a shock tunnel environment. To allow a direct comparison, the strain gage balance of Marineau et al. [4] was modified by replacing flexures with piezoelectric load cells for the same 6-in. Apollo capsule geometry.

Presented as Paper 2011 at the 49th AIAA Aerospace Sciences Meeting, Orlando, FL, 4–7 January 2011; received 7 February 2011; accepted for publication 14 February 2011. Copyright © 2011 by CUBRC. Published by the American Institute of Aeronautics and Astronautics, Inc., with permission. Copies of this paper may be made for personal or internal use, on condition that the copier pay the $10.00 per-copy fee to the Copyright Clearance Center, Inc., 222 Rosewood Drive, Danvers, MA 01923; include the code 0022-4650/11 and $10.00 in correspondence with the CCC.

*Senior Research Scientist. Member AIAA.

II. New Piezoelectric Force Balance

The new six-inch-diameter Apollo capsule balance uses three PCB Piezotronic Inc. piezoelectric load cells located as shown in Fig. 1a , where each load cell is sensitive to forces in three orthogonal directions with intrinsic small linear interactions and large stiffness. Because of the increased distance between the force transducers, the sensitivity to the pitching moment is increases compared with traditional sting mounted balances. Using a linear interaction model, the force and moments are related to the measured force transducers and accelerometers outputs as

$$F(t)_j^T = (S_F(t)_i^T + S_A(t)_k^T C_{A_{ki}})C_{F_{ij}} \quad \text{for } i = 1 \ldots N_S$$
$$j = 1 \ldots N_C; \qquad k = 1 \ldots N_A \tag{1}$$

where summation is performed over repeated indices. The static calibration was performed at the 13 calibration points shown in Fig. 1a to obtain $\mathbf{C_F}$. Details about the calibration process are found in Marineau et al [4]. The balance was calibrated for three components, namely axial force (x-direction), normal force (y-direction), and pitching moment for the convention shown in Fig. 1b. Since the piezoelectric balance does not have a true dc response, the calibration is performed by suddenly removing weights at the various calibration points. The static response is then obtained by averaging the dynamic response over several oscillation cycles to obtain the steady load. This time period was long enough to include a sufficient number of cycles to remove the effects from the sting vibrations and short enough compared with the time constant of the piezoelectric sensors.

Results for axial loads applied at point "a" (directly located below load cell $1T$) are shown in Fig. 2a, where the excellent linearity from both the main output and interaction terms are seen. For this particular load case, an ideal balance would only show an output in the z-direction for load cell $1T$ ($S1T_z$ output). However, significant outputs are seen in the other directions for all the sensors. Crosstalk arises because of internal forces in this statically overdetermined structure. As expected, the sum of those outputs scaled by the respective sensitivities and sensor orientation is equal to zero as it should be for internal forces. Even if the crosstalk is significant, reliable measurements were obtained as the crosstalk terms are linear and can be effectively remove using the interaction matrix. The linear least-square fit detailed in Marineau et al. [4] was used to obtain the interaction matrix. The calibration error for a 95% confidence interval ($\pm 3\sigma$) was 0.2 lbf for the normal force, 1.4 lbf for the axial force, and 2.4 lbf-in. for the pitching moment. It was also verified that the crosstalk was successfully removed with the interaction matrix. The interaction in the normal direction due to a force in the axial direction was reduced to 0.2% compared with 2% for that in the axial direction due to a force in the normal direction. The normal-due-to-axial crosstalk is of greater concern since the axial force is typically 10 times the normal force for a capsule at angle-of-attack (AOA). However, due to small level of interaction, the error is not expected to be greater than 2% (0.2% × 10). Also, since the calibration uncertainties are estimated with large point loads as opposed to a distributed load (corresponding to smaller discrete point loads) in the actual

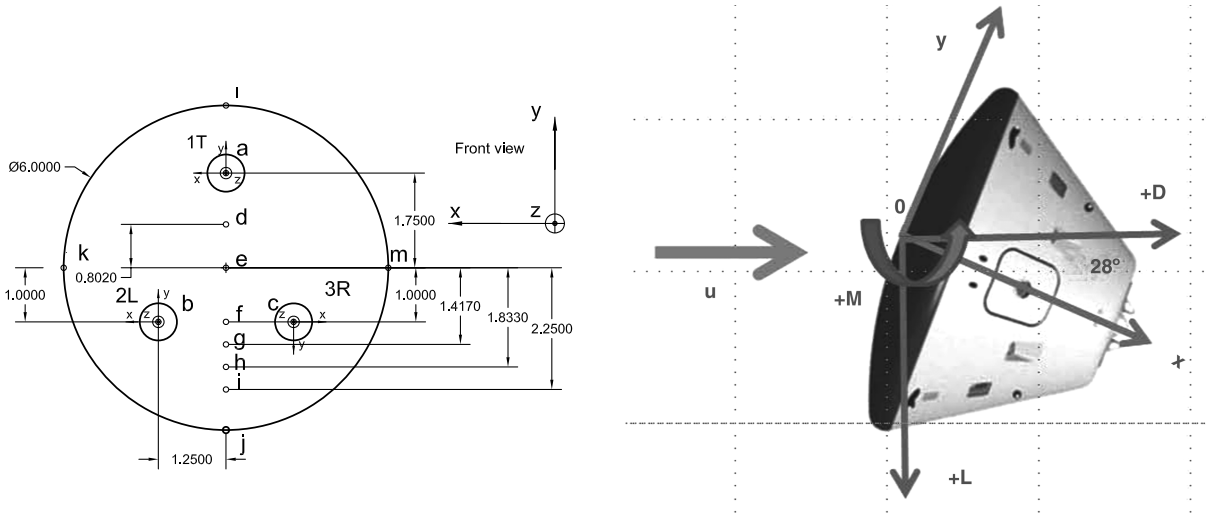

a) Calibration points **b) Force and moments convention**

Fig. 1 Balance geometry and convention for force and moments.

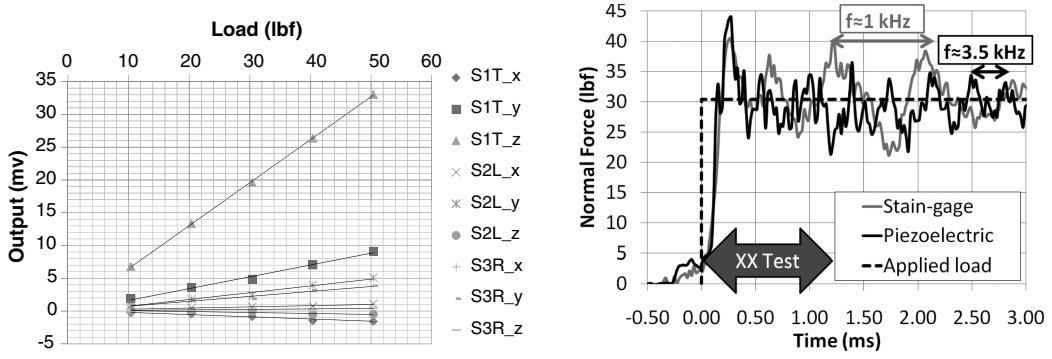

a) Static calibration **b) Acceleration compensation**

Fig. 2 Typical results for the static calibration showing good linearity and acceleration compensation showing improved frequency response over strain gage balance.

testing, the computed error is expected to be a conservative estimate of the actual error as nonlinearities increase with load magnitude.

The inertial loads can be removed by measuring the acceleration of the model and by performing a dynamic calibration to determine the effective inertial mass of the model-balance assembly $\mathbf{C_A}$. Details about the dynamic calibration methodology are presented in Marineau et al. [4]. For that particular balance design, the output needs to be compensated for the bending and compression modes of the sting. A step load is generated as described in Marineau et al. [4] and the accelerations measured with accelerometers. The scaling factors are determined using a linear least-square fit to remove the inertial loads. A typical result for the dynamic calibration is seen in Fig. 2b along with that of the strain gage balance [4]. A significant increase in the frequency response of the balance is seen compared with the previous balance design.

III. Experimental Setup and Test Conditions

Data were acquired at 75 kHz using the Diversified Technical Systems, Inc. onboard data acquisition system providing 32 channels with 16 bit A/D conversion. To validate the new balance, a total of 3 runs were performed in the 48 in. tunnel at two test conditions (C1 and C2 [4]). One run was performed for each condition at 0-deg AOA and one run at 28-deg AOA for condition C1. The test conditions computed with Candler's nozzle code [7] are found in Table 1.

IV. Experimental Results

To validate the new balance, measurements were compared with that by Marineau et al. [4] and Data Parallel Line Relaxation (DPLR) [8] computational fluid dynamics (CFD) simulations at the same nominal test conditions. Details about the CFD methodology are found in Marineau et al. [4]. Raw traces at 0 deg AOA for conditions C1 and C2 are shown in Fig. 3. Excellent agreement for the axial force is seen between the piezoelectric balance and the strain gage balance. One also notices the higher natural frequencies of the piezoelectric balance compared with the strain gage balance. Both forces balances yield average values of C_A within 1% of each other and within 1.5% of the CFD prediction for both test conditions. Figures 4a and 4b present C_A, C_N, and C_M comparisons between the

Table 1 Test conditions

Condition	Tunnel	M_∞	u_∞, m/s	p_∞ Pa	ρ_∞, kg/m^3	T_∞, K	Tv_∞, K	q_∞, Pa	h_0, MJ/kg	cN2	cO2	cNO	cN	cO	cAr
C1	48-Inch	9.3	1287	176	0.0125	49	1248	10333	0.8	1.000	0.000	0.000	0.000	0.000	0.000
C2	48-Inch	9.3	1305	544	0.0573	49	1248	48754	0.9	1.000	0.000	0.000	0.000	0.000	0.000

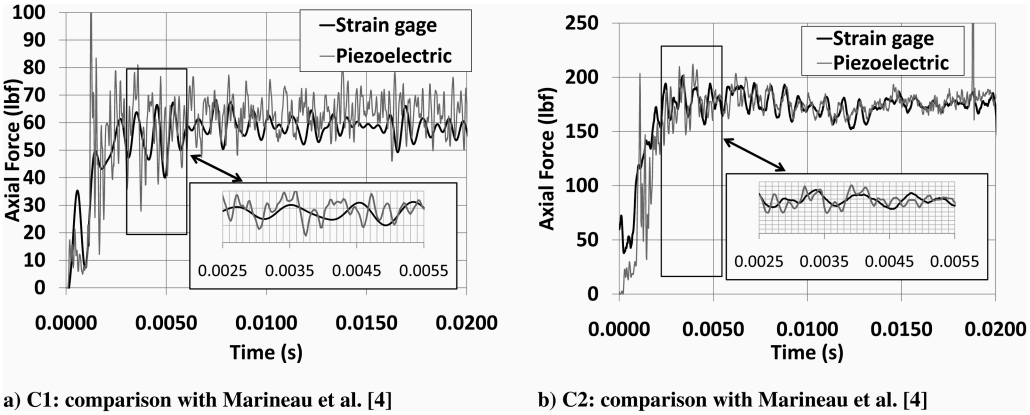

a) C1: comparison with Marineau et al. [4] b) C2: comparison with Marineau et al. [4]

Fig. 3 Axial force at 0-deg AOA.

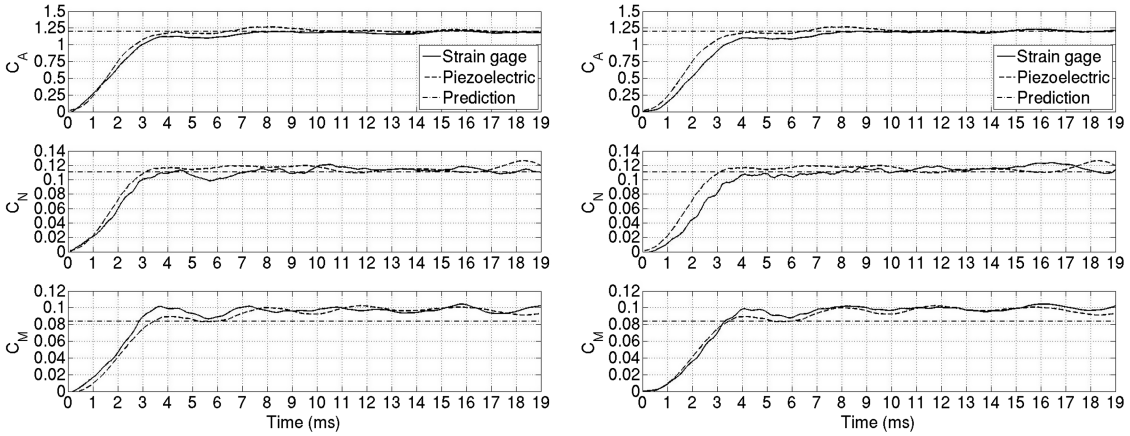

a) C1: Comparison with run 3 of Marineau et al. [4] b) C1: Comparison with run 6 of Marineau et al. [4]

Fig. 4 Force coefficient at 28-deg AOA for condition C1.

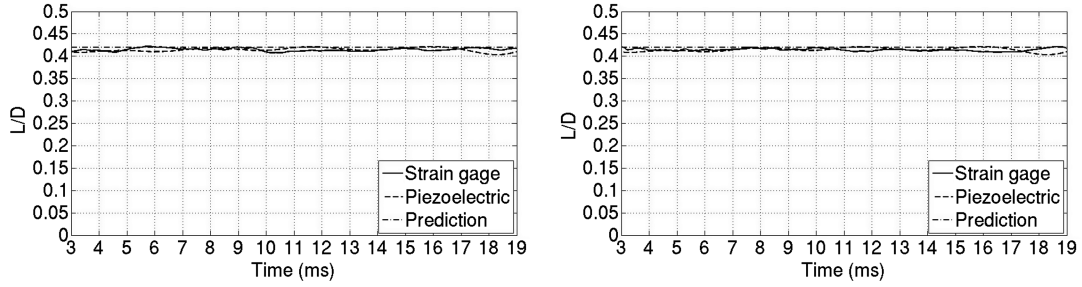

a) C1: Comparison with run 3 of Marineau et al. [4] b) C1: Comparison with run 6 of Marineau et al. [4]

Fig. 5 Lift-to-drag ratio L/D for condition C1.

piezoelectric balance and two runs with the strain gage balance [4] at 28-deg AOA for the same nominal C1 test condition. Here, an eight-pole low-pass Butterworth filter with cutoff frequencies of 0.5 and 1 kHz were used, respectively, for the strain gage and piezoelectric balance signals. Comparison for L/D are found in Fig. 5 and numerical results are tabulated in Table 2. The fluctuations in the C_A, C_N, and C_M traces are due to fluctuations in the pitot pressure. When plotting L/D, the fluctuations are greatly reduced as the effect of the variation in the free stream dynamic pressure is removed. Here, the standard deviation in L/D is less than for 1% for both balances. The two balances yields values of C_A within 2% of each other. Excellent agreement between the measured and predicted C_A is also seen as the difference is less than 1%. Both balances overpredict the pitching

Table 2 Force coefficients at 28-deg AOA compared with strain gage balance and CFD prediction

C_A piezo	C_A strain gage	C_A CFD	$\Delta_{ps}C_A$, %	$\Delta_{CFD}C_A$, %
1.189	1.211	1.200	−1.8	−0.9
C_N piezo	C_N strain gage	C_N CFD	$\Delta_{ps}C_N$ %	$\Delta_{CFD}C_N$ %
0.116	0.107	0.111	7.8	5.3
C_M piezo	C_M strain gage	C_M CFD	$\Delta_{ps}C_M$ %	$\Delta_{CFD}C_M$ %
0.088	0.095	0.084	−7.9	5.1
L/D piezo	L/D strain gage	L/D CFD	$\Delta_{ps}L/D$ %	$\Delta_{CFD}L/D$ %
0.412	0.418	0.420	−1.4	−1.8

moments (compared with CFD). The piezoelectric balance produces a 5% increase over the numerical prediction.

V. Conclusions

This paper has shown that accurate force measurements can be obtained in shock tunnels with an acceleration compensated piezoelectric force balance. The new methodology using an array of triaxial piezoelectric load cells yields a stiff, sensitive, and accurate design. More precisely, the new balance displays a 350% increase in frequency response over a conventional strain gage balance [4] with a similar level of accuracy and a 400% increase in sensitivity. The calibration process has shown an excellent linearity in the principal outputs and for the interaction terms, which implies that they can be removed using a linear interaction model. The accuracy of the balance was demonstrated through comparison with measurements on the same capsule model equipped with internal flexures and strain gages instead of the piezoelectric sensors. Values of L/D for both balances were within 1.4% of each other and within 1.8% of the CFD prediction. The new piezoelectric balance agrees within 5% of the numerical prediction for C_A, C_N, and C_M. The new force measurement technology will be used to build improved force balances for use in the LENS-XX shock tunnel on reentry capsules and slender configuration such as winged entry vehicle and hypersonic cruise vehicles.

Acknowledgments

The work presented in this paper was performed with funding from CUBRC internal research and U.S. Air Force Office of Scientific Research Grant No. N00244-09-1-0060. The author is also grateful to Michael Holden for providing the internal research opportunity and to the entire LENS crew for the hard work on tunnel operation, instrumentation and mechanical design during this project.

References

[1] Schoenenberger, M., Dyakonov, M., Buning, A., Scallion, P., Norman, W., and Van, J., "Aerodynamic Challenges for the Mars Science Laboratory Entry, Descent and Landing," AIAA Paper 2009-3914, 2009.

[2] Storkmann, V., Olivier, H., and Gronig, H., "Force Measurements in Hypersonic Impulse Facilities," *AIAA Journal*, Vol. 36, No. 3, 1998, pp. 342–348. doi:10.2514/2.402

[3] Laurence, S., and Karl, S., "An Improved Visualization-Based Force-Measurement Technique for Short-Duration Hypersonic Facilities," *Experiments in Fluids*, Vol. 48, No. 6, 2009, pp. 949–965. doi:10.1007/s00348-009-0780-9

[4] Marineau, E., MacLean, M., Mundy, E., and Holden, M., "Force Measurements in Hypervelocity Flows with an Acceleration Compensated Strain Gage Balance," AIAA Paper 2011-951, 2011.

[5] Schewe, G., and Steinho, C., "Force Measurements on a Circular Cylinder in a Cryogenic Ludwieg-Tube Using Piezoelectric Transducers," *Experiments in Fluids*, Vol. 42, No. 3, 2007, pp. 489–494. doi:10.1007/s00348-007-0250-1

[6] Norman, A., "Effect of Surface Morphological Changes on Flow over a Sphere," Ph.D. Thesis, California Inst. of Technology, 2010.

[7] Candler, G., "Hypersonic Nozzle Analysis Using an Excluded Volume Equation of State," AIAA Paper 2005-5202, 2005.

[8] Wright, M., Bose, D., and Candler, G., "A Data Parallel Line Relaxation Method for the Navier–Stokes Equations," *AIAA Journal*, Vol. 36, No. 9, 1998, pp. 1603–1609. doi:10.2514/2.586

M. Miller
Associate Editor